

PAPER

Effect of few-layer MoS₂ flakes deposited ZnO/FTO nanorods on photoelectrochemical characteristic

To cite this article: Tien Dai Nguyen *et al* 2019 *Mater. Res. Express* **6** 085070

View the [article online](#) for updates and enhancements.




IOP | ebooks™

Bringing you innovative digital publishing with leading voices to create your essential collection of books in STEM research.

Start exploring the collection - download the first chapter of every title for free.



PAPER

Effect of few-layer MoS₂ flakes deposited ZnO/FTO nanorods on photoelectrochemical characteristicRECEIVED
9 February 2019REVISED
27 April 2019ACCEPTED FOR PUBLICATION
9 May 2019PUBLISHED
24 May 2019Tien Dai Nguyen¹ , Minh Tan Man¹, Manh Hung Nguyen², Dong-Bum Seo³ and Eui-Tae Kim³¹ Institute of Theoretical and Applied Research, Duy Tan University, Hanoi 100000, Vietnam² Department of Materials Science and Engineering, Le Quy Don Technical University, Hanoi 100000, Vietnam³ Department of Materials Science and Engineering, Chungnam National University, Daejeon 34134, Republic of KoreaE-mail: nguyentidai@duytan.edu.vnKeywords: ZnO nanorod, MoS₂-flake, photoelectrochemical, hybrid nanostructure**Abstract**

We report on photoelectrochemical (PEC) characteristic of a few-layer MoS₂-flakes deposited ZnO nanorod (MS-ZNR) configuration prepared via the hydrothermal and the metal-organic chemical vapor deposition (MOCVD) approach. The MS-ZNR nanostructure exhibited enhanced photo-excited electron-hole pair separation and transfer for energy-storage/or conversion applications. Due to a suppressing the recombination mechanism of charge carriers, the PEC performance of MS-ZNR photoelectrode revealed higher photocurrent density (1.42 mA.cm⁻² at 0.2 V, $\eta = 0.91\%$, with 0.1 M Na₂S electrolyte) than a ZnO NR photoelectrode. We propose a potential application of MoS₂-flakes hybrid nanostructure as enhanced efficient, inexpensive, and non-noble metal for PEC devices.

1. Introduction

Photoelectrochemical (PEC) material research for water splitting has been interesting as a promising solution to produce high hydrogen gas efficiency, inexpensive and environment friendless to replace the conventional fossil fuels [1–3]. Multi-structured semiconductors (TiO₂, ZnO), as well as two-dimensional (2D) transition-metal dichalcogenide (MX₂, M=Mo, W, Ti, V, and X=S, Se, Te) have been extensively studied to promise the PEC photoanodes. They have exhibited highly photoexcited electron-hole pair separation and transfer, excellent chemical stability, and earth abundance. Moreover, many efforts have been widely investigated to semiconductor photocatalysts for achieving water to hydrogen conversion efficiency. Especially, molybdenum disulfides (MoS₂) have received significant attention in a recent year because of its potential applications in optoelectronic devices [4–7]. High mobility of the few-layer MoS₂ is fast separation and transfer of charge carriers, an excellent combination between large/flexible areas, and controllable bandgap (from 1.2–1.9 eV) [8, 9] due to quantum confinement effects. At present, MoS₂ has been successfully reported by many approaches, including micromechanical exfoliation [8, 10], metalorganic chemical vapour deposition (MOCVD) [4, 11], mechanical exfoliation [8, 12], hydrothermal [4, 13], solvothermal [14], liquid phase exfoliation [7], laser ablation [15]. Among them, the MOCVD method is the simplest vapor phase technique to synthesize few-layer MoS₂ flake, typically in a large and flexible area. Besides, pure zinc oxide (ZnO) material based water splitting researches have been indicated a good promising heterogeneous photoelectrochemical. It exhibited attracted properties such as photoexcited electron-hole in visible light, contribution with many homogeneous photocatalysts, high carrier mobility, low cost [16]. However, ZnO has still exhibited many limitations due to fast recombination of charge carriers, and a wide band gap (3.37 eV) to photoexcitation in visible light for improving photoelectrochemical efficient of ZnO. To obtain high photoelectrochemical efficient, many efforts have been reported to modify pristine ZnO structure, in which has used doping noble metals (Au, Ag, Pt) [17, 18], hybrid, and composite nanostructure [5, 19, 20].

In this work, we studied an effect of the few-layer MoS₂-flakes deposited ZnO NR structure on morphological, optical, structural properties. Furthermore, the PEC cell was also investigated using 0.1 M Na₂S buffer with sulfuric acid (H₂SO₄) electrolyte in the potential range between –0.6 to 0.4 V.

2. Experimental procedures

A vertically-standing ZnO nanorod array was grown on a 500-nm-thick fluorine doped tin oxide (FTO) glass substrate by the hydrothermal route [21, 22] in a Teflon-lined stainless steel autoclave. First, a 200-nm-thick Zn film was deposited on FTO substrate by the direct current (DC) magnetron sputtering method (power of 50 watts, a target-substrate distance of 10-cm, and time of 1 min). The zinc film was treated by a temperature at 500 °C for 2 h in the air to form a ZnO seed-mediated hydrothermal method. Second, an aqueous solution of zinc nitrate (0.04 M, $(\text{Zn}(\text{NO}_3)_2, 0.91 \text{ g}; \text{H}_2\text{O}, 60 \text{ ml})$) and hexamethylenetetramine (0.04 M, $\text{C}_2\text{H}_{12}\text{N}_4, 0.67 \text{ g}; \text{H}_2\text{O} 60 \text{ ml}$) (from Sigma Aldrich Inc.) was dissolved for ZnO nanorod growth. After the synthesis, the ZNR array was annealed at 500 °C for 2 h in the air with 8 °C min^{-1} of ramping time. A few-layer MoS_2 flake was deposited on ZnO nanorod array using MOCVD system at 200 °C under pressure of 1 mTorr. A precursor of Mo and S as $\text{Mo}(\text{CO})_6$ (vaporized at 20 °C) and H_2S (75 sccm of flow rate, 5% in balance N_2), respectively was conducted in a quartz tube using an Ar gas of 25 sccm [6, 23]. The morphology of an MS-ZNR sample was investigated by field emission scanning electron microscope (FE-SEM, energy-dispersive X-ray (EDX) techniques (Hitachi, Japan S-4800). By using the X-ray diffraction (XRD) technique ($\text{Cu}_K\alpha$ radiation, $\lambda = 1.54 \text{ \AA}$, Rigaku), micro Raman, spectroscopy (ANDOR) using an exciting wavelength of 532-nm, the structural properties of the MS-ZNR were studied. Also, a Fourier-transform infrared spectroscopy (FTIR-5700) was used to investigate the infrared reflectance property of the MS-ZNR structure. The working size of a PEC cell was processed in a $0.5 \times 0.5 \text{ cm}^2$ of FTO glass substrate using epoxy to cover an undesired area. A three electrode system (Pt sheet as counter and KCl saturated calomel $\text{Hg}/\text{Hg}_2\text{Cl}_2$ as reference electrodes), electrochemical analyzer (potentiostat/galvanostat 263 A), electrolyte comprised of 0.1 M Na_2S buffer with H_2SO_4 , a 150 W Xe arc lam solar simulator with AM 1.5 G filter ($100 \text{ mW}\cdot\text{cm}^{-2}$ of power), and sourceMeter (Keithley 2400) were used for PEC characterization.

3. Results and discussion

FE-SEM images of few-layer MS-ZNR flake samples with different deposition times (60, 90 and 120 s) are shown in figures 1(b)–(d). As deposited MoS_2 on ZnO NRs, the thick MoS_2 layer is continued growth while deposition time is increased and its covered the whole surface of ZnO NRs, as shown in figure 1(d).

The morphology of vertical-standing ZnO NR was significantly affected by the MoS_2 amount, which was modified the ZnO NR shape from a smooth side-well to flake. The diameter of ZnO NRs also was manipulated from 50 to 70-nm after 120 s. The edge of the MoS_2 flake is grown on the side-well of ZnO NR that exhibited more conductive than a basal plane. For the 60 s, the morphology of the ZnO NR did not change significantly compared with the pristine ZnO/FTO substrate, as shown in figure 1(b). This structure has been provided better electric contact and high efficiency of photogenerated electrons and holes process for the PEC water splitting application [6, 7, 23, 24].

The MS-ZNR structures were confirmed through the XRD and EDS spectra, as shown in figures 2 and 3. The XRD peaks at $2\theta = 31.749^\circ, 34.420^\circ, 36.230^\circ, 47.526^\circ, 56.544^\circ, 62.855^\circ, 67.918^\circ, 69.01^\circ, 72.56^\circ, \text{ and } 76.920^\circ$ that are assigned to the (100), (002), (101), (102), (110), (103), (112), (201), (004), and (202) planes of hexagonal wurtzite of ZnO (Ref. JCPDS No. 036-1451), respectively. Comparing with a pristine ZnO NR, XRD peak at $2\theta = 14.19^\circ$ is also assigned to the (002) plane of a hexagonal phase of MoS_2 (Ref. JCPDS No. 037-1492) [25]. Although there is not different morphology between pristine ZnO NR and MS-ZNR (as-deposited of the 60 s) samples. However, the MS-ZNR is still observed diffraction peak at the (002) plane with a strong intensity that is characterized by a good crystal structure of MoS_2 flakes. The intensity of (002) MoS_2 plane is also increased by the increasing growth time. In figure 3, the EDX spectrum of the point shape scanning of the MS-ZNR array (120 s) that shown clearly observed Zn, O, Mo, S element peaks. The elemental concentrations are obtained as 31.35, 66.14, 0.95, and 1.56% in weight of oxygen, zinc, sulfide, and molybdenum, respectively. The result exhibits a purity of MS-ZNR structure without other elements. In figure 4, Raman spectra of the ZnO nanorod and few-layer MoS_2 deposited ZNR samples are shown. Phonon frequency peaks at 95.8, 202.6, 276.6, 322.7, 376.9, 434.8, 538, and 579.7 cm^{-1} correspond to the modes of $E_2^{\text{low}}, 2E_2^{\text{low}}, B_1^{\text{low}}, 2E_2, E_2^{\text{high}}, A_1(\text{TO}), B_1^{\text{high}}$, and $1E_1$ (LO), respectively. Also, E_{1g}, E_{2g}^1 , and peaks are attributed to phonon variation frequencies of hexagonal MoS_2 at 284.2, 378.09, and 405.04 cm^{-1} , respectively. The A_g^1 and peaks are assigned to the out-of-plane and in-plane modes that come from a variation of the atomic S-Mo, and S modes [25, 26], respectively. To explain the vibration of ZnO modes, the optical phonons Γ_{opt} is given by $\Gamma_{\text{opt}} = 1A_1 + 2B_1 + 1E_1 + 2E_2$ [26]. Herein, $A_1, E_1, \text{ and } 2E_2$ ($E_2^{\text{low}}, E_2^{\text{high}}$) modes are a transverse optical mode (TO), a longitudinal optical mode (LO and frequency vibration phonon of an oxygen atom, and heavy Zn sublattices, respectively. Besides, the $2B_1$ ($B_1^{\text{low}}, B_1^{\text{high}}$) modes are Raman active by conducting defects [26]. Fourier transform infrared spectroscopy (FTIR) of MS-ZNR samples were carried out at room temperature in the range of 850–3600 cm^{-1} , as shown in

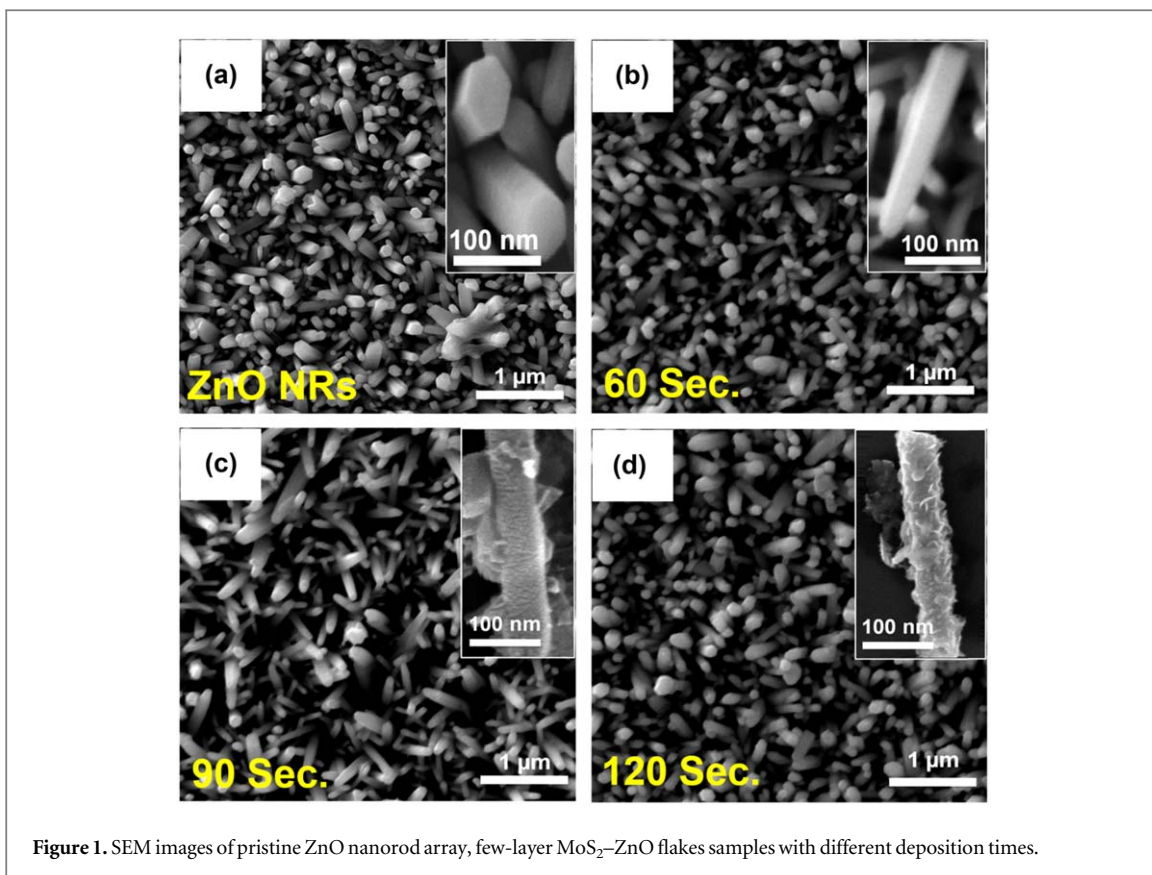


Figure 1. SEM images of pristine ZnO nanorod array, few-layer MoS₂-ZnO flakes samples with different deposition times.

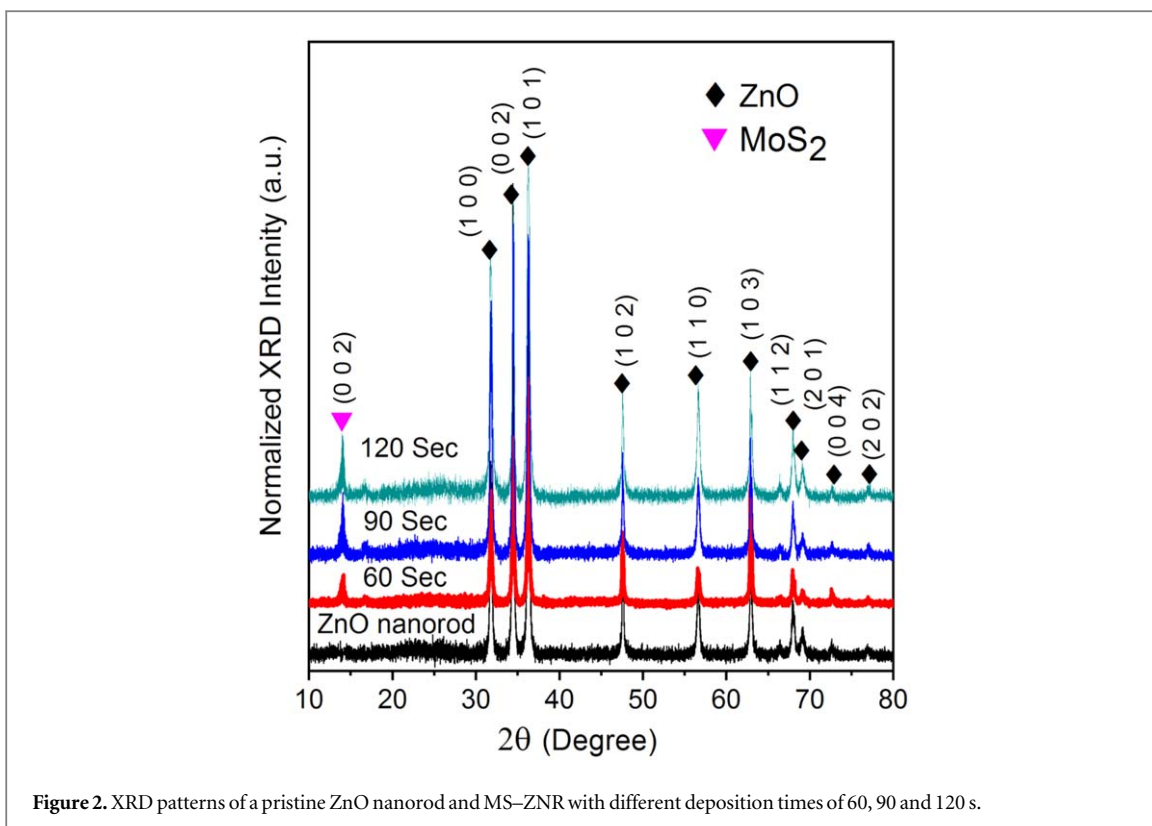


Figure 2. XRD patterns of a pristine ZnO nanorod and MS-ZNR with different deposition times of 60, 90 and 120 s.

Figure 5. The result showed that the spectral reflectance of samples is as a function of wavenumber and as well as a surface roughness (nanorods).

The samples have stronger sensitivity and absorption in short IR range (2000–3500 cm⁻¹) than mid-IR-range (1000–2000 cm⁻¹). Most samples absorb IR radiation at about 1021, 1405, 1632, 2184, 2810 and

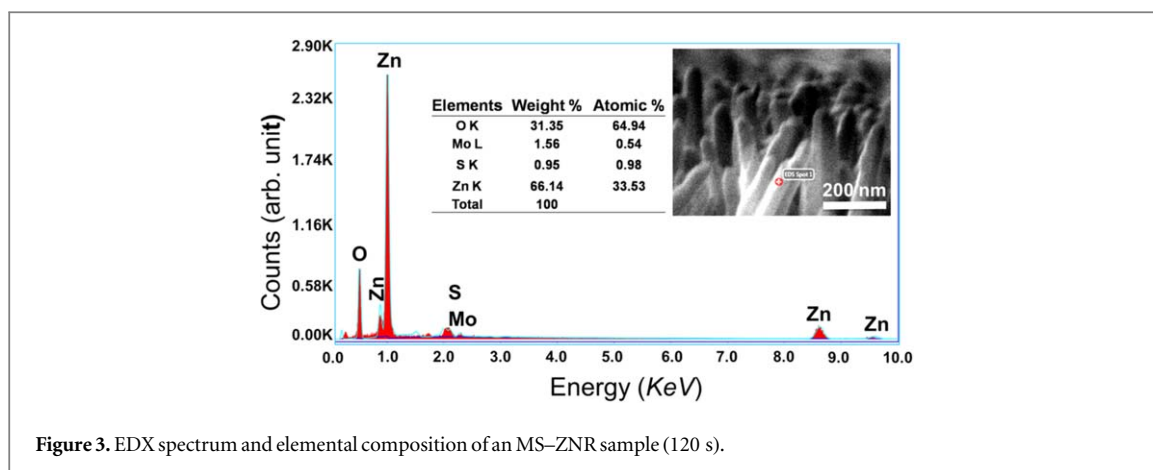


Figure 3. EDX spectrum and elemental composition of an MS-ZNR sample (120 s).

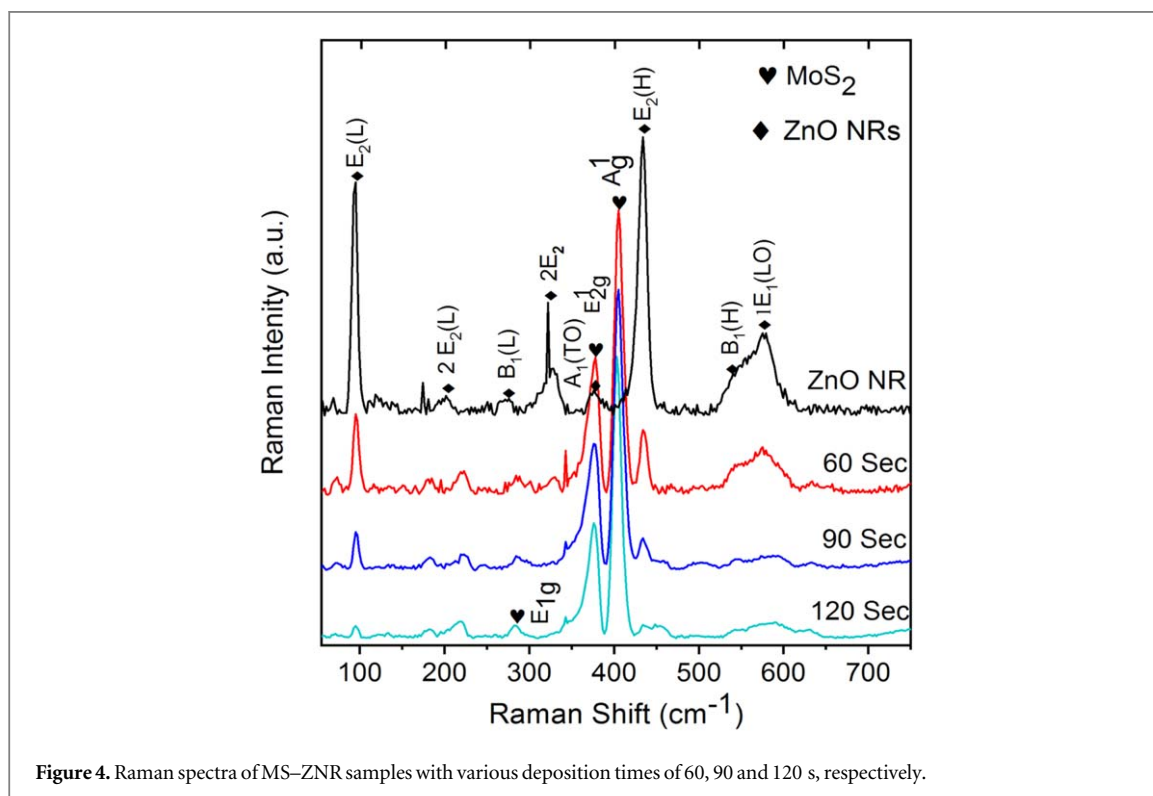
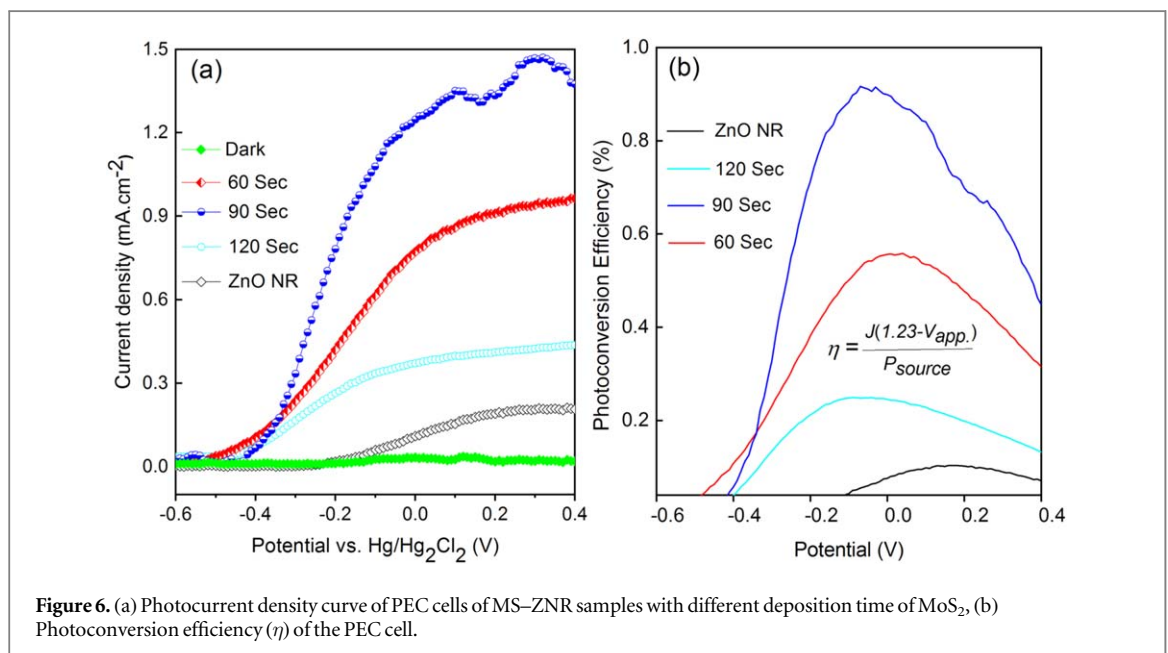
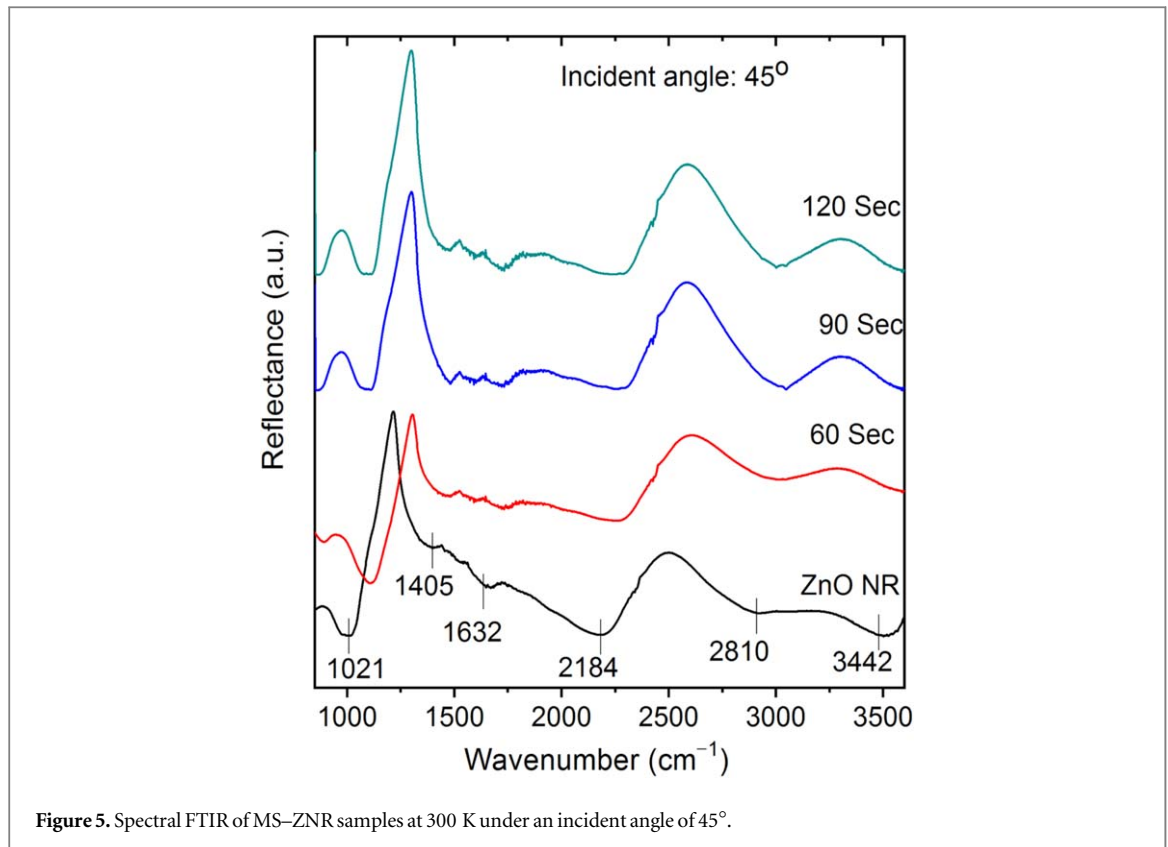


Figure 4. Raman spectra of MS-ZNR samples with various deposition times of 60, 90 and 120 s, respectively.

3442 cm^{-1} in the IR range that corresponds to ZnO nanorod [27, 28]. Comparing to pristine ZnO NR that less absorbs than MS-ZNR. The MS-ZNRs also reveal a blue-shift at about 1405 cm^{-1} due to a rough morphology effect of nanorod (a few-layer MoS_2 flakes).

As a result, we determined the few-layer MoS_2 flakes completely deposited ZnO/FTO nanorod which could be further applied for a photoelectrochemical (PEC) cell. The PEC cell was investigated in dark and under UV-light in the potential range between -0.6 to 0.4 V at a scan rate of $10\text{ mV}\cdot\text{s}^{-1}$ using a $0.1\text{ M Na}_2\text{S}$ buffer with H_2SO_4 electrolyte, as shown in figure 6(a). The photocurrent density (PCD) strongly depended on as-deposited MoS_2 content. The MS-ZNR (90 s) sample revealed a maximum current of a $1.42\text{ mA}\cdot\text{cm}^{-2}$ at an applied potential of 0.2 V , while ZnO NR sample exhibited the PCD of a $0.2\text{ mA}\cdot\text{cm}^{-2}$ at 0.2 V . However, the PCD ($0.43\text{ mA}\cdot\text{cm}^{-2}$ at 0.2 V) of the MS-ZNR (120 s) sample is less than a $0.99\text{ mA}\cdot\text{cm}^{-2}$ comparing to the MS-ZNR (90 s) sample at the same condition. Figure 6(b) shows photoconversion efficiency (η) of the PEC cell with various working electrodes. The device obtained a maximum value of 0.56% , at -0.05 V , 0.91% at -0.07 V , and 0.25% at -0.08 V for MS-ZNR samples with 60, 90 and 120 s, respectively. The PEC cell promotes high photocatalytic efficiency due to a fast photogenerated electron-hole pair separation, and transfer properties across the heterojunction. The more MoS_2 content deposition could further promote adhesive MoS_2 -to-ZnO (type II-like). The reducing the surface area in contact with the electrolyte that leads to a reduced electrochemical property occurring at the surface, thus, reducing the photocurrent density.



Besides, thicker MoS₂-flake will absorb more photons yielding more photogenerated electron-hole pairs, the transport distance of a carrier to the output circuit also increased. It implies decreasing PEC efficiency due to a recombination loss. Also, the length diffusion of a carrier should be larger than a distance between heterojunction and the edge of MoS₂-flakes [23, 29], and thus, the high of the MoS₂ flakes should be less than 200-nm. Vertically-standing MoS₂ not only served as a higher area of the edge per unit substrate area but also established better electronic contact with ZnO nanorods. This result leads to enhancing PCD up to seven times (1.42 mA.cm⁻²) more than that of only ZnO NRs (0.2 mA.cm⁻²). Beyond this finding, we propose a potential application of MoS₂-flakes hybrid nanostructure as highly efficient, inexpensive for photoelectrochemical applications.

4. Conclusions

In summary, we successfully synthesized a vertically-standing few-layer MoS₂/ZnO/FTO nanorod for improving photoelectrochemical (PEC) cell performance using MOCVD approach. Various deposited time of MoS₂-flakes that critically affected PEC performance. The PEC performance of MoS₂/ZnO/FTO (90 s) sample obtained a photocurrent density of a 1.42 mA.cm⁻² at 0.2 V with 7 times higher than that of pristine ZnO NRs. This result base on a high density of their edge and fast photogenerated electron-hole pair separation and transfer mechanism across the heterojunction. As a result, we recommend a hybrid way that combines hydrothermal, and MOCVD growth to further promote the photoelectrochemical activity of ZnO by employing non-noble metal MoS₂ catalyst.

Acknowledgments

This research was partially supported by Nano. Material Technology Development Program through the National Research Foundation of Korea (NRF) funded by the Ministry of Science, ICT, and Future Planning (2009-0082580) and The Institute of Theoretical and Applied Research (ITAS), Duy Tan University, Hanoi 100000, Vietnam.

ORCID iDs

Tien Dai Nguyen  <https://orcid.org/0000-0002-9420-210X>

References

- [1] Ding Q *et al* 2016 Efficient electrocatalytic and photoelectrochemical hydrogen generation using MoS₂ and related compounds *Chem* **1** 699–726
- [2] Han B and Hu Y H 2016 MoS₂ as a co-catalyst for photocatalytic hydrogen production from water *Energy Sci. Eng.* **4** 285–304
- [3] Chen B *et al* 2018 Preparation of MoS₂/TiO₂ based nanocomposites for photocatalysis and rechargeable batteries: progress, challenges, and perspective *Nanoscale* **10** 34–68
- [4] Xiaoli Z 2014 A review: the method for synthesis MoS₂ monolayer *Int. J. of Nanomanufacturing* **10** 489–99
- [5] Li H *et al* 2018 MoS₂ nanosheet/ZnO nanowire hybrid nanostructures for photoelectrochemical water splitting *J. Am. Ceram. Soc.* **101** 3989–96
- [6] Trung T N *et al* 2018 Enhanced photoelectrochemical activity in the heterostructure of vertically aligned few-layer MoS₂ flakes on ZnO *Electrochim. Acta* **260** 150–6
- [7] Ji S *et al* 2013 Exfoliated MoS₂ nanosheets as efficient catalysts for electrochemical hydrogen evolution *Electrochim. Acta* **109** 269–75
- [8] Mak K F *et al* 2010 Atomically thin MoS₂: a new direct-gap semiconductor *Phys. Rev. Lett.* **105** 136805
- [9] Park J W *et al* 2014 Optical properties of large-area ultrathin MoS₂ films: evolution from a single layer to multilayers *J. Appl. Phys.* **116** 183509
- [10] Splendiani A *et al* 2010 Emerging photoluminescence in monolayer MoS₂ *Nano Lett.* **10** 1271–5
- [11] Endler I *et al* 1999 Chemical vapour deposition of MoS₂ coatings using the precursors MoCl₅ and H₂S *Surf. Coat. Technol.* **120–121** 482–8
- [12] Novoselov K S *et al* 2005 Two-dimensional atomic crystals *Proc. Nat. Acad. Sci. USA* **102** 10451–3
- [13] Li W-J *et al* 2003 Hydrothermal synthesis of MoS₂ nanowires *J. Cryst. Growth* **250** 418–22
- [14] Feng X *et al* 2013 Novel mixed-solvothermal synthesis of MoS₂ nanosheets with controllable morphologies *Cryst. Res. Technol.* **48** 363–8
- [15] Compagnini G *et al* 2012 Monitoring the formation of inorganic fullerene-like MoS₂ nanostructures by laser ablation in liquid environments *Appl. Surf. Sci.* **258** 5672–6
- [16] Tian N *et al* 2016 Utilization of MoS₂ nanosheets to enhance the photocatalytic activity of ZnO for the aerobic oxidation of benzyl halides under visible light *Ind. Eng. Chem. Res.* **55** 8726–32
- [17] He L *et al* 2014 Fabrication of Au/ZnO nanoparticles derived from ZIF-8 with visible light photocatalytic hydrogen production and degradation dye activities *Dalton Trans.* **43** 16981–5
- [18] Tian-you P *et al* 2011 Preparation of ZnO nanoparticles and photocatalytic H₂ production activity from different sacrificial reagent solutions *Chin. J. Chem. Phys.* **24** 464
- [19] Liang P *et al* 2015 Doping properties of MoS₂/ZnO (0001) heterojunction ruled by interfacial micro-structure: from first principles *Solid State Commun.* **204** 67–71
- [20] Benavente E *et al* 2018 Heterostructured layered hybrid ZnO/MoS₂ nanosheets with enhanced visible light photocatalytic activity *J. Phys. Chem. Solids* **113** 119–24
- [21] Greene L E *et al* 2003 Low-temperature wafer-scale production of ZnO nanowire arrays *Angew. Chem.-Int. Ed.* **115** 3139–42
- [22] Greene L E *et al* 2005 General route to vertical ZnO nanowire arrays using textured ZnO seeds *Nano Lett.* **5** 1231–6
- [23] Seo D-B *et al* 2019 Conformal growth of few-layer MoS₂ flakes on closely-packed TiO₂ nanowires and their enhanced photoelectrochemical reactivity *J. Alloys Compd.* **770** 686–91
- [24] He H *et al* 2016 MoS₂/TiO₂ edge-on heterostructure for efficient photocatalytic hydrogen evolution *Adv. Energy Mater.* **6** 1600464
- [25] Feng G *et al* 2015 Synthesis of flower-like MoS₂ nanosheets microspheres by hydrothermal method *J. Mater. Sci. Mater. Electron.* **26** 8160–6
- [26] Musa I, Qamhieh N and Mahmoud S T 2017 Synthesis and length dependent photoluminescence property of zinc oxide nanorods *Results Phys.* **7** 3552–6

- [27] Anžlovar A *et al* 2012 Polyol-mediated synthesis of zinc oxide nanorods and nanocomposites with poly(methyl methacrylate) *J. Nanomaterials* **2012** 9
- [28] Khun K *et al* 2014 A selective potentiometric copper (II) ion sensor based on the functionalized ZnO nanorods *J. Nanosci. Nanotechnol.* **14** 6723–31
- [29] Kim Y C *et al* 2018 Evaluation of transport parameters in MoS₂/graphene junction devices fabricated by chemical vapor deposition *ACS Appl. Mater. Interfaces* **10** 5771–8